

II. MICROWAVE GASEOUS DISCHARGES*

Prof. S. C. Brown
Prof. W. P. Allis
Prof. D. R. Whitehouse
Dr. G. Bekefi
Dr. L. Mower
C. D. Buntschuh

J. D. Coccoli
S. Frankenthal
R. B. Hall
R. L. Hall
J. L. Hirshfield

W. R. Kittredge
J. J. McCarthy
W. J. Mulligan
G. B. Nichols
Judith L. Shaver
C. S. Ward

RESEARCH OBJECTIVES

The aim of this group continues to be to study some of the fundamental properties of gas discharge physics by means of microwave plasmas, with more and more emphasis on high-density plasmas and plasmas in magnetic fields. To carry out this general objective, we have spent a great deal of effort on the production of plasmas of high-percentage ionization at low pressures under steady-state conditions, the achievement of which will allow us to carry on the fundamental studies in which we are most interested. At the present time, we have not produced plasmas with as high percentage of ionization as we had hoped to, but we have several schemes under way for producing them.

We are also studying ways of determining the characteristics of plasmas by means of microwaves, spectroscopic methods, and the diamagnetic effect of electrons. Along with these production and diagnostic studies, we are continuing measurements on fundamental physics studies of loss and gain mechanisms of the electrons in the plasmas. Considerable emphasis is being put on studying the microwave radiation from plasmas, with and without magnetic fields, both as a tool for measuring the plasma temperature and as a means of understanding more about the motion of ions and electrons in a magnetic field.

S. C. Brown

A. MICROWAVE NOISE RADIATION FROM PLASMAS

We previously reported (1) results of preliminary measurements of the microwave noise emitted from a cylindrical column of a helium plasma. We indicated that the observed variations of the emission with electron density and with gas pressure can be interpreted on the basis of the absorptivity which the plasma presents to the radiation. In this report we outline the computations that were made for comparison with the measurements. Experiments on magnetized plasmas will also be discussed.

The problem of computing the amount of radiation emitted by a plasma requires a knowledge of the emission and absorption coefficients at every point (x, y, z) within the medium. In general, only one of these coefficients is known; the other is obtained by assuming that the plasma is everywhere in thermodynamic equilibrium. This assumption allows us to relate the absorption and emission through Kirchhoff's law, which states that for an isotropic medium

$$\eta_{\nu}(x, y, z) = \alpha_{\nu}(x, y, z) \mu^2(x, y, z) B(x, y, z; \nu, T) \quad (1)$$

* This work was supported in part by the Atomic Energy Commission under Contract AT(30-1)1842.

(II. MICROWAVE GASEOUS DISCHARGES)

Here η_ν is the emissivity per unit volume of plasma at a frequency ν ; a_ν is the absorption coefficient per unit path length within the plasma; B is the intensity of the equilibrium radiation per unit frequency interval, determined by the radiation temperature T of the medium; and μ is the refractive index of the plasma. Subject to Eq. 1 and subject to the assumption that the plasma temperature is constant throughout its volume (i. e., with B independent of x, y, z), the intensity of I_ν of the radiation emitted in the direction \vec{s} is found (2) to be

$$I_\nu(x, y, z; \nu, \vec{s}) = B(\nu, T)[1 - e^{-\tau}] \quad (2)$$

where τ , the optical thickness, is given by

$$\tau = \int a_\nu(x, y, z) ds$$

The integration is to be carried out over the complete trajectory of the ray within the plasma.

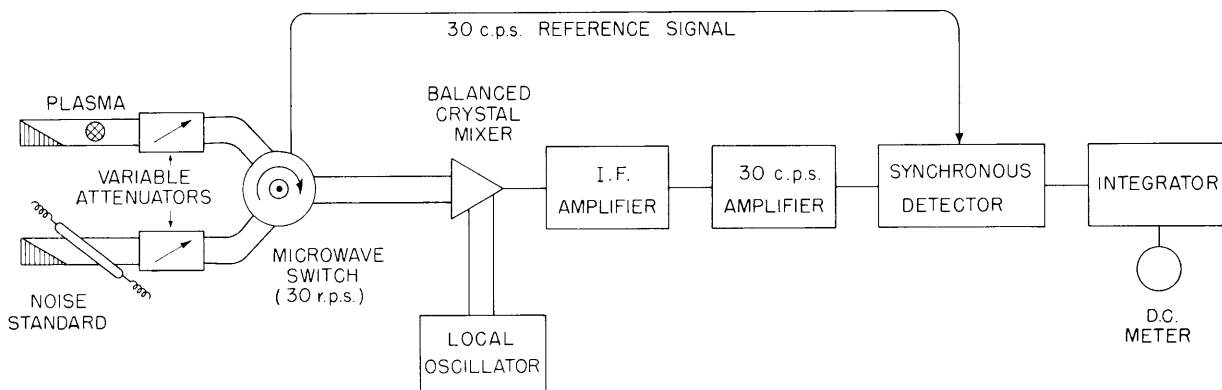


Fig. II-1. Schematic diagram of a 3000-mc radiometer.

In the present experiment the noise radiation comes from a section of a cylindrical plasma column, 7.5 cm long, with radius $R = 1.2$ cm; the column traverses at right angles the narrow side of a rectangular S-band waveguide (Fig. II-1). In computing the radiation intensity from Eq. 2, the ray trajectories are taken to lie along the direction of propagation of the waveguide mode. The total noise power E_ν in the frequency interval $d\nu$ is obtained by integrating I_ν over the cross section of the waveguide. With the aid of the fact (1, 3) that in the limit $a_\nu \rightarrow \infty$ (completely opaque plasma) the noise power

(II. MICROWAVE GASEOUS DISCHARGES)

traveling down the waveguide is kT , we arrive at the value E_ν for the available noise from a semiopaque or transparent plasma:

$$E_\nu(a, T) = kT \frac{1}{R} \int_0^R (1 - e^{-\tau(\rho)}) d\rho$$

$$\tau(\rho) = 2 \int_\rho^R a(r)(r^2 - \rho^2)^{-1/2} r dr$$
(3)

Here r represents the radius vector with its origin at the center of the plasma column. The attenuation coefficient $a(r, \theta, z)$ is assumed to vary only in the r direction.

The attenuation coefficient is a function of the frequency ν , of the electron density n , and of the collision frequency for momentum transfer $\nu_m(\nu)$ of an electron of average velocity v with the other particles in the plasma. Our plasma is of a low degree of ionization (less than 0.1 per cent) and collisions are therefore predominantly with neutral particles. Furthermore, ν_m in helium is nearly independent of electron energy for energies in excess of approximately 2 eV; ν_m has a value of $2.4 \times 10^9 p_0 \text{ sec}^{-1}$, where p_0 is the gas pressure normalized to 0° C . Hence, subject to the assumption of a constant collision frequency, the attenuation coefficient, as computed on the basis of plane wave propagation in an infinite medium, has the form (4)

$$a(r) = \frac{\sqrt{2}\pi}{\lambda} \left\{ \left(\frac{(1-\gamma)^2 + \beta^2}{1 + \beta^2} \right)^{1/2} - \left(1 - \frac{\gamma}{1 + \beta^2} \right) \right\}^{1/2}$$
(4)

where λ is the wavelength; β is the ratio of collision frequency to the radian frequency (ν_m/ω); $\gamma = (n(r)e^2/m\epsilon_0\omega^2)$ is the square of the ratio of the plasma frequency to the radian frequency.

For the purpose of evaluating $a(r)$, the electron density distribution over the cross section of the plasma column is assumed to vary as $n(r) = n_0 J_0(2.405 r/R)$, where $J_0(x)$ is a Bessel function of the first kind. This assumption is reasonable for gas pressures in excess of approximately 0.1 mm Hg, at which pressures the tube diameter exceeds the electron mean-free path by a factor of 10 or more. At low electron densities ($\gamma \ll 1$) the attenuation coefficient is directly proportional to the electron density, so that $a(r)$ exhibits the same variation with r as $n(r)$ does. For the sake of simplifying the computations, we assumed a Bessel-function dependence for $a(r)$ also at higher electron densities ($\gamma \approx 1$). Some discrepancies (particularly at the lower gas pressures) between experiment and theory which were observed in the neighborhood of electron densities of $\gamma \approx 1$ are believed to be the result of the approximations. More exact computations are being made.

(II. MICROWAVE GASEOUS DISCHARGES)

Figures II-2 and II-3 show the results of measurements and computations. The former are represented by dots, the latter by solid lines. On the ordinate the ratio E_v/kT in decibels is plotted, for a constant T equal to that measured at the black-body limit ($a \rightarrow \infty$); on the abscissa the central electron density n_0 is plotted. The arrow marked n_p refers to a density n_0 for which $\gamma = 1$.

The noise measurements were supplemented by measurements of the voltage standing-wave ratio (VSWR) for a wave propagating in the direction of the plasma. The VSWR is then used to correct for the fact that the plasma impedance is not matched to the waveguide impedance and that only a fraction of the total available noise power E_v is received. At electron densities lower than approximately $5 \times 10^{10} \text{ cm}^{-3}$, the correction for the noise power is less than 0.2 db, and at higher densities it never exceeds 3 db. In several cases of low electron densities, departures from linearity between E_v/kT and n_0 were observed (see, for example, Fig. II-1, gas pressure 9.4 mm Hg, indicated by a dashed line). These departures are attributed to changes of the electron temperature with density during this particular run. This is substantiated by the fact that in these cases the measured electric field \mathcal{E} along the positive column also showed marked changes with n_0 . Such departures were observed only at pressures in excess of 2 mm Hg.

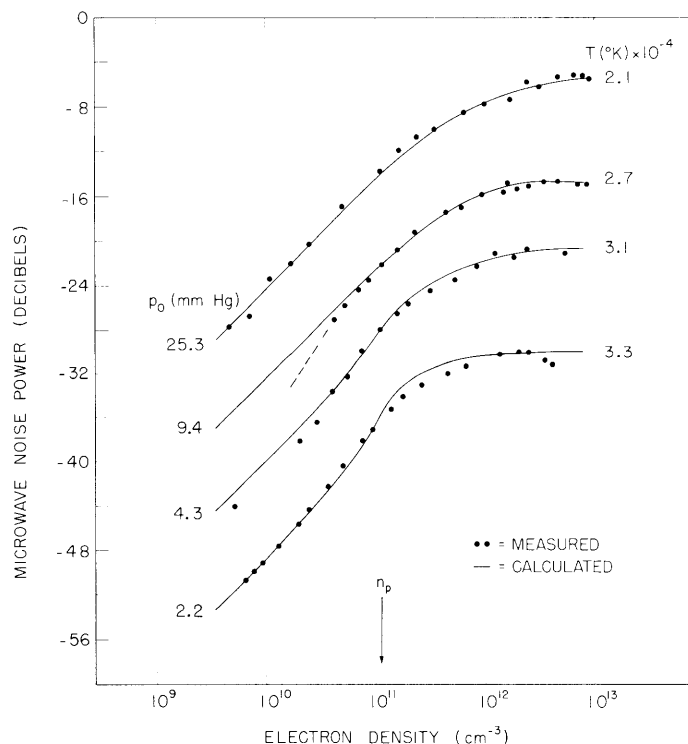


Fig. II-2. Microwave noise power versus the electron density for gas pressures from 25 to 2 mm Hg. The measured radiation temperature, T , is also given.

(II. MICROWAVE GASEOUS DISCHARGES)

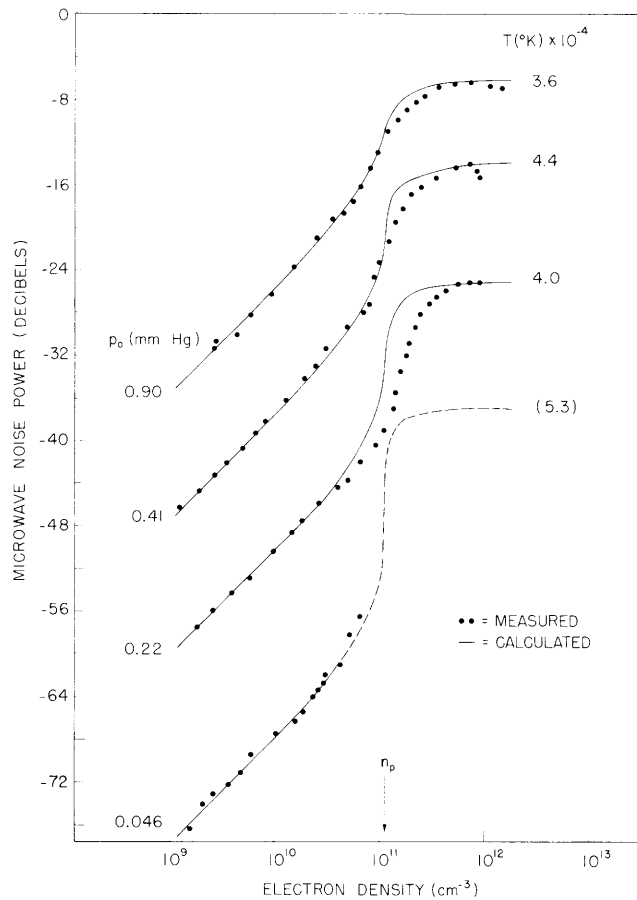


Fig. II-3. Microwave noise power versus the electron density for gas pressures from 0.9 to 0.05 mm Hg.

The knowledge of the variation of T with \mathcal{E}/p_0 can be used to bring the calculations into harmony with measurements.

These observations lead us to believe that the radiation temperature T of an isotropic plasma can be deduced with fair accuracy even though the black-body limit ($a \rightarrow \infty$) is not reached; provided that (a) the electron density is known with precision, (b) the density distribution is known approximately, and (c) the collision processes are understood so that a can be calculated.

Radiation from magnetized (anisotropic) plasmas is considerably more difficult to interpret than that from isotropic plasmas. The propagation and attenuation constants are now functions of direction relative to the applied magnetic field, and Eqs. 1 and 2 are no longer applicable in their simple form (5). Furthermore, additional sources of radiation, such as cyclotron and Čerenkov radiation, are possible (6). Preliminary measurements are shown in Fig. II-4 for a uniform dc magnetic field B applied along the axis of the plasma column. The electric field of the radiated microwave noise is

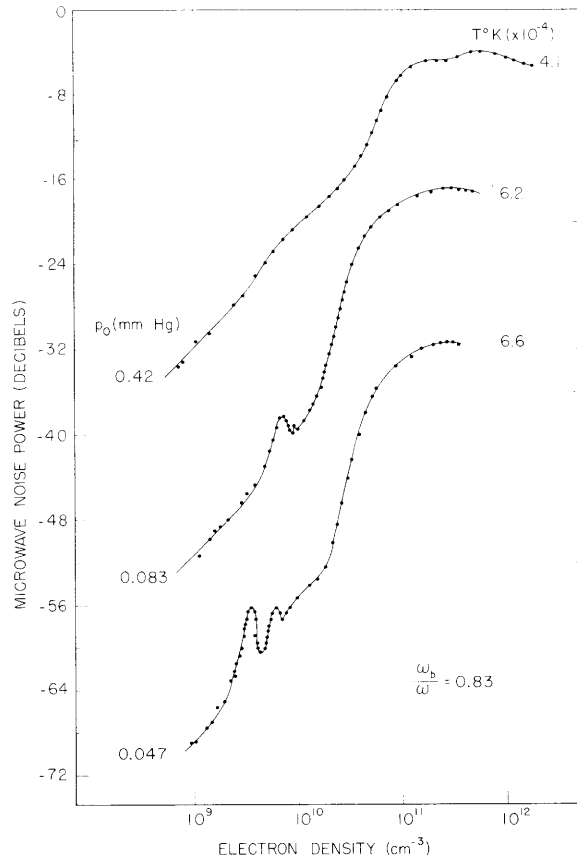


Fig. II-4. Microwave noise power versus the electron density for a magnetized plasma. The constant dc magnetic field is applied along the plasma column.

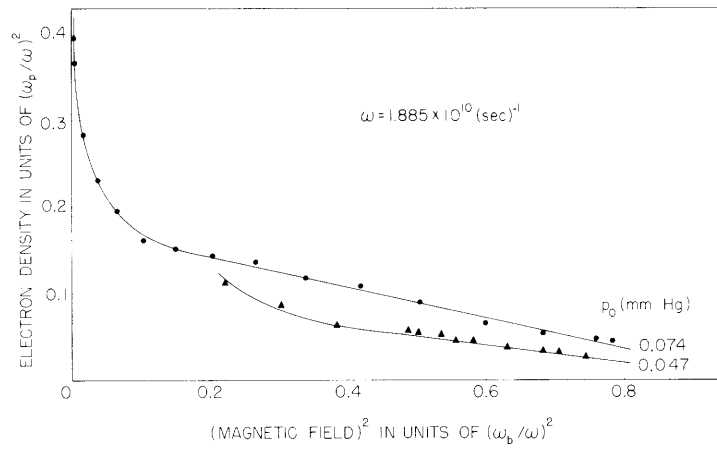


Fig. II-5. Variation of the resonance maximum as a function of the magnetic field and of the electron density. The curves refer to the more pronounced resonance shown in Fig. II-4.

(II. MICROWAVE GASEOUS DISCHARGES)

measured perpendicular to B. The measurements shown in Fig. II-4 are for a fixed magnetic field $(\omega_p/\omega) = eB/m\omega = 0.83$. The appearance of resonances with decreasing gas pressure will be noted.

When the magnetic field is increased, the resonances move to a lower electron density. This is shown in Fig. II-5; here the position of the more pronounced peak (corresponding to the one situated at lower electron density in Fig. II-4) is plotted against magnetic field. It is suggested that the resonances are associated with the resonance absorption suffered by the extraordinary wave in its passage through the anisotropic plasma. However, the results of Fig. II-5 are not in quantitative agreement with computations based on propagation perpendicular to B in an infinite anisotropic medium.

G. Bekefi, J. L. Hirshfield

References

1. G. Bekefi and J. L. Hirshfield, Quarterly Progress Report No. 51, Research Laboratory of Electronics, M.I.T., Oct. 15, 1958, p. 8.
2. R. V-D. R. Wooley, Supplement to Austr. J. Sci. 10, No. 2 (1947).
3. P. Parzen and L. Goldstein, Phys. Rev. 82, 724 (1951).
4. S. J. Buchsbaum, Ph.D. Thesis, Department of Physics, M.I.T., 1957.
5. F. V. Bunkin, J.E.T.P. (Soviet Physics) 5, 665 (1957).
6. V. Ia. Eidman, J.E.T.P. (Soviet Physics) 34(7), 91 (1958).

B. RF PLUGS FOR DISCHARGES IN A MAGNETIC FIELD

Magnetic mirrors have been considered extensively for the reflection of particles moving along magnetic-field lines. One disadvantage of the mirror scheme is that particles that lie within the "escape cone" of the configuration will not be reflected back into the discharge region but will be lost to the vessel walls.

A less familiar containment device is the microwave cavity. Because of the gradients of the electromagnetic field in the cavity, time-averaged forces are exerted on charged particles. In addition, the presence of a static magnetic field leads to a resonance of the time-average force when the cavity frequency is near the cyclotron frequency. The derivation of the time-average force \bar{f} is straightforward, and only the results are given here.

$$\bar{f} = \frac{1}{2} \text{Re}[(\bar{p} \cdot \nabla) \mathbf{E}^* + \bar{p} \times (\nabla \times \mathbf{E}^*)] \quad (1)$$

The symbol Re means "the real part of." The dipole moment \bar{p} of a single particle is defined as the product of the charge q and the vector displacement \bar{r} of the particle oscillating in the field about its equilibrium position.

(II. MICROWAVE GASEOUS DISCHARGES)

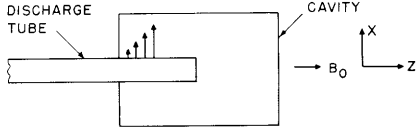


Fig. II-6. Electromagnetic plug.

For simplicity, a simple dc magnetic field and ac electromagnetic field configuration will be considered in order to demonstrate the reflection properties of the device (Fig. II-6).

1. Electromagnetic Plug

A cavity is chosen with the electric field \bar{E} in the x-direction and with the static magnetic field B_0 in the z-direction. In this case, the dipole moment of the particles will be at right angles to the variation of electric field, so that the first term within brackets in Eq. 1 equals zero. The dipole moment $\bar{p} = q\bar{r}$ is determined by the solution of the equation of motion. The result, for the simple geometry that we have chosen, is

$$p_x = \frac{e^2}{2j\omega m} [\ell + r] E_x \quad (2)$$

where

$$\ell = \frac{1}{\nu_c + j(\omega + \omega_b)}; \quad r = \frac{1}{\nu_c + j(\omega - \omega_b)} \quad (3)$$

ν_c = collision frequency for momentum relaxation

$$\omega_b = \frac{eB}{m} \quad (4)$$

Substitution of Eq. 2 in Eq. 1 yields

$$\bar{f} = \frac{e^2}{4m\omega} \operatorname{Re} \left[\left(\frac{\ell + r}{j} \right) E_x \frac{\partial E_x^*}{\partial z} \bar{i}_z \right] \quad (5)$$

With substitution of Eq. 3 in Eq. 5 and simplification of the results, we have

$$\bar{f} = \left(-\frac{1}{4} \frac{e^2}{m\omega^2} \frac{\partial E_x^2}{\partial z} \bar{i}_z \right) \left[\frac{1 - \left(\frac{\omega_b}{\omega} \right)^2 + \left(\frac{\nu_c}{\omega} \right)^2}{\left(1 - \left(\frac{\omega_b}{\omega} \right)^2 - \left(\frac{\nu_c}{\omega} \right)^2 \right)^2 + 4 \left(\frac{\nu_c}{\omega} \right)^2} \right] \quad (6)$$

The term in parentheses in Eq. 6 represents the force exerted on a charged particle in the absence of a magnetic field. It is observed that the direction of this force reflects particles traveling in the positive z-direction. The term within brackets in Eq. 6 has a behavior that gives a large force amplification near resonance. The amplification

(II. MICROWAVE GASEOUS DISCHARGES)

factor (brackets) will be called M , and the magnetic field for resonance will be determined.

$$M = \frac{\eta - \xi}{(\eta + \xi)^2 + 4\eta} \quad (7)$$

$$\eta = \frac{v^2}{\omega^2}, \quad \xi = \left(\frac{\omega_b}{\omega}\right)^2 - 1 \quad (8)$$

The optimum gain is found by differentiating M with respect to ξ , with η treated as a constant. The result is

$$\xi_{\text{opt}} = \eta \pm 2(\eta^2 + \eta)^{1/2} \quad (9)$$

In practice, the ratio of collision frequency to applied frequency is very small, so that Eq. 9 can be simplified to yield

$$\xi_{\text{opt}} \approx \pm 2(\eta)^{1/2} \quad (10)$$

The maximum gain, M_{opt} , is determined by substituting Eq. 9 in Eq. 7. Thus

$$M_{\text{opt}} = \frac{\mp 1}{4[(\eta^2 + \eta)^{1/2} \pm \eta]} \quad (11)$$

In the approximation of small collision frequencies Eq. 11 reduces to

$$M_{\text{opt}} = \frac{1}{4(\eta)^{1/2}} \quad (12)$$

$$\xi_{\text{opt}} = -2(\eta)^{1/2}$$

Although the gain, M_{opt} , indicated in Eqs. 12 may be very large for small collision frequencies, it is necessary to consider the bandwidth of the resonance because of the practical necessity of controlling the magnetic field within fine tolerances.

The bandwidth of the resonance is defined as the width of the region in which $M \geq \frac{1}{2} M_{\text{opt}}$. The value of $\xi = \xi_{1/2}$ at the half-gain points is given approximately by

$$\xi_{1/2} = \eta^{1/2}[-4 \pm 2\sqrt{3}] \quad (13)$$

It is seen from Eqs. 13 and 12 that the curve of M versus ξ is not symmetric

(II. MICROWAVE GASEOUS DISCHARGES)

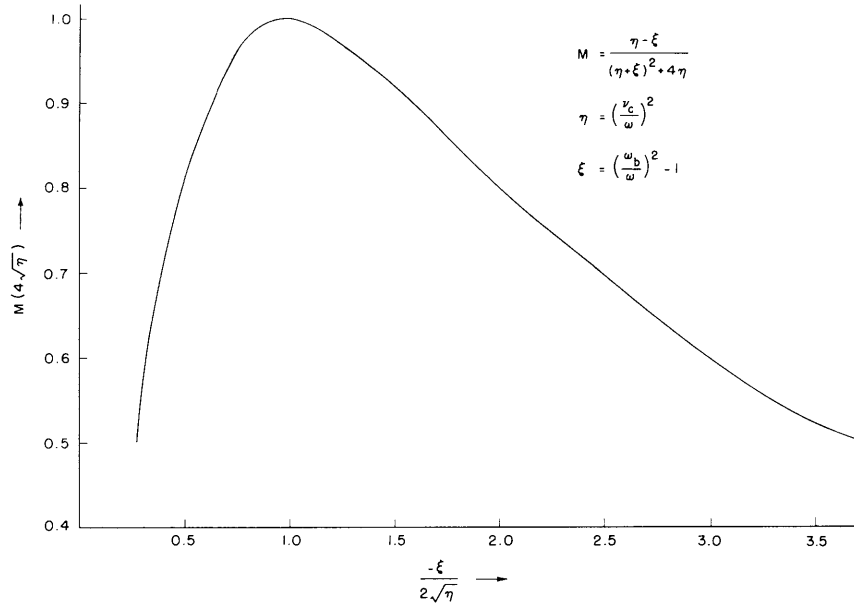


Fig. II-7. Magnetic-field resonance curve.

about the value ξ_{opt} . The normalized curve of M versus ξ is shown in Fig. II-7.

The bandwidth $\Delta\xi_{1/2}$ is found from Eq. 13

$$\Delta\xi_{1/2} = \eta^{1/2} 4\sqrt{3} = 4\sqrt{3} \frac{v_c}{\omega} \quad (14)$$

The bandwidth $\Delta(\omega_b)_{1/2}$ is found by substituting Eq. 8 in Eq. 14

$$\Delta(\omega_b)_{1/2} = 2\sqrt{3} v_c \quad (15)$$

Similarly, the bandwidth of the magnetic field $\Delta B_{1/2}$ (in MKS units) is

$$\Delta B_{1/2} = \frac{2\sqrt{3}}{(e/m)} v_c \quad (16)$$

For hydrogen, the collision frequency is given approximately by $v_c = 5.9 \times 10^9$ p. Thus

$$\Delta B_{1/2} \text{ (gauss)} = 1.2 \times 10^3 p \quad (17)$$

with p in mm Hg.

Instead of asking for the bandwidth for $M = (1/2) M_{\text{opt}}$, it is useful to inquire about the bandwidth at a low gain, for example, $M = (1/100) M_{\text{opt}}$. In this case

$$\Delta B_{1/100} \text{ (gauss)} = 6.9 \times 10^4 p \quad (18)$$

(II. MICROWAVE GASEOUS DISCHARGES)

We see from the arguments given above that a useful gain M can be obtained by operating the magnetic field near cyclotron resonance. The particle energies V which can be reflected from the cavity plugs are easily shown to be

$$V(\text{volts}) = \frac{Me}{4m\omega^2} E_{x\text{max}}^2 \quad (19)$$

where M is the resonance term that has been discussed. The maximum value of the electric field $E_{x\text{max}}$ is the important parameter of the cavity, as seen from Eq. 19. The maximum reflected particle energy is thus proportional to M , the microwave power, and the cavity Q .

R. B. Hall

C. PLASMA AND SHEATH POTENTIALS IN LOW-PRESSURE MICROWAVE DISCHARGES

For low-pressure microwave cavity discharges in a magnetic field (see Quarterly Progress Report, Oct. 15, 1957, p. 3) the end walls of the quartz tube container become negatively charged, and an electrostatic potential well or sheath is produced. The following experiment has been performed to determine the potential across this end-wall sheath by analysis of the ions that arrive at the end wall. At low pressures, when the ion mean-free path is long, the ion energy will be equal to the potential through which they have fallen.

Figure II-8 shows a drawing of the experimental quartz tube that was used in the analysis of the ion energies. The tube diameter is 0.5 inch in the discharge region, and it has a hole of 40-mil diameter centrally located in one end. The ions and electrons stream out of the small hole along the magnetic field lines and encounter an electrode structure consisting of a grid and a cylindrical cup. The potential applied to these electrodes establishes an E-field along the magnetic field. Thus the current to the cup is a function of the axial energy of the particles and the potential difference, V , between the electrodes.

Hydrogen gas fills the entire glass enclosure and a plasma is produced in the quartz

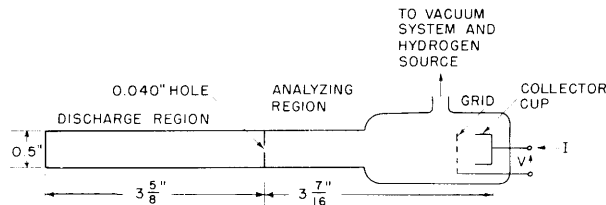


Fig. II-8. Experimental tube in axial energy analyzer.

(II. MICROWAVE GASEOUS DISCHARGES)

tube by microwave methods. The externally applied magnetic field is uniform in the discharge region and diverges to 90 per cent of its value at the position of the analyzing electrodes.

When the applied voltage V is positive (positive cup), the current density to the cup is given by

$$J_{\text{cup}} = -n_+ e \int_V^\infty f_+(u_z) v_{z+} du_z + n_- e \int_0^\infty f_-(u_z) v_{z-} du_z \quad \text{for } V > 0 \quad (1)$$

with the axial distribution function normalized so that

$$\int f(u_z) du_z = 1$$

Equation 1 shows that all of the electrons are collected but only those ions with axial energy greater than V are collected. For a high-density beam, it is assumed that $n_+ = n_- = n$, and in the steady state the electron and ion currents must be equal. Therefore

$$J_{\text{cup}} = ne \left[- \int_V^\infty f_+(u_z) v_{z+} du_z + V_{z+} \right] = ne \int_0^V f_+(u_z) v_{z+} du_z \quad (2)$$

By differentiating Eq. 2 with respect to the voltage V it is possible to obtain directly the axial ion distribution function.

$$\frac{d}{dV} J_{\text{cup}} = \frac{d}{dV} \int_0^V ne f_+(u_z) \left[\frac{2eu_z}{M} \right]^{1/2} du_z = ne f_+(V) \left[\frac{2eV}{M} \right]^{1/2} \quad (3)$$

It therefore follows from Eq. 3 that

$$f_+(V) = \frac{1}{ne} \left[\frac{M}{2eV} \right]^{1/2} \frac{d}{dV} J_{\text{cup}} \quad \text{for } V > 0 \quad (4)$$

For hydrogen discharges below 1μ , Eq. 4 will properly predict the ion energy distribution. At higher gas pressures, the degradation of ion energy caused by collisions will shift the distribution to lower energies.

Analysis of the current for a negative cup has not been made because the reflected electrons can stream back into the discharge tube and upset the assumption of equal currents from the tube.

Typical plots of I versus V are shown in Fig. II-9a and 9b for low and high pressures, respectively. The breaks in the curve at energies marked V_s and V_p indicate

(II. MICROWAVE GASEOUS DISCHARGES)

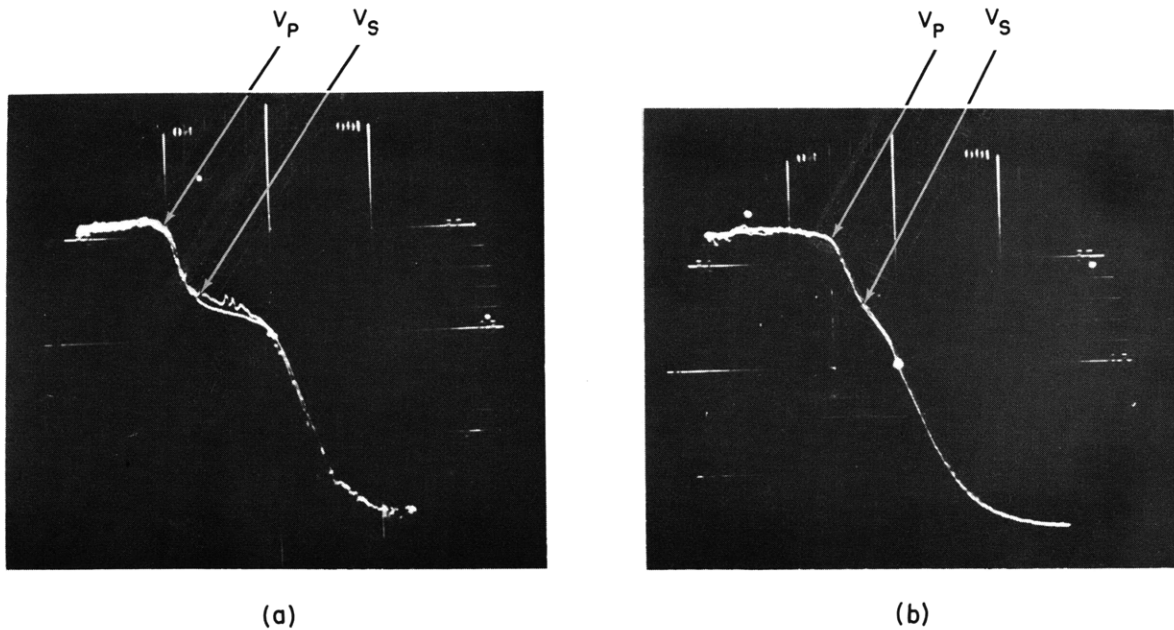


Fig. II-9. Cup current versus voltage: (a) low pressure; (b) high pressure.

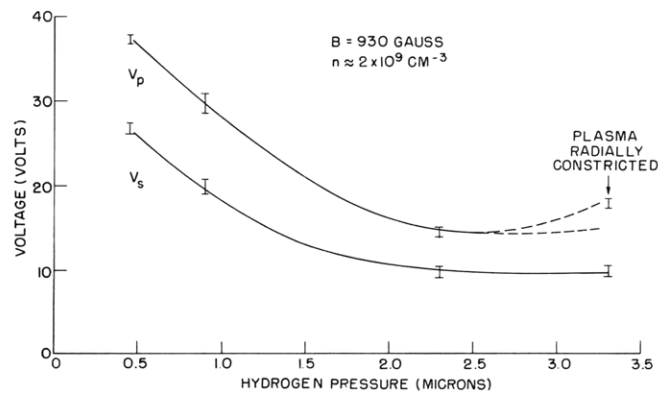


Fig. II-10. Plasma and sheath potentials versus pressure.

the potential across the sheath and the plasma potential at the center of the tube. Differentiation of this curve would show that most of the ions have an energy between V_S and V_P . Thus an ion that is generated inside the tube will accelerate and strike the end wall with an energy between V_S and V_P which will depend on its position at birth.

The plasma and sheath potentials were measured as a function of pressure. The data plotted in Fig. II-10 were taken with a magnetic field of 930 gauss, a relatively constant electron density, and constant microwave excitation frequency. At any given

(II. MICROWAVE GASEOUS DISCHARGES)

pressure, there was only a small variation of V_p and V_s with electron density.

It is concluded from the experimental data that the space-charge potential is maximum in the center of the tube, falls 5 to 10 volts at the edge of the axial sheath, and then falls another 10 to 20 volts across the sheath. The potentials V_p and V_s increase as the pressure is decreased, which is consistent with the necessity for better electron containment at lower pressures.

D. R. Whitehouse, Judith L. Shaver, J. D. Coccoli